Fractal analysis of canard cycles with two breaking parameters and applications

Peer-reviewed author version

HUZAK, Renato & Vlah, Domagoj (2019) Fractal analysis of canard cycles with two breaking parameters and applications. In: COMMUNICATIONS ON PURE AND APPLIED ANALYSIS, 18 (2), p. 959-975.

DOI: 10.3934/cpaa.2019047
Handle: http://hdl.handle.net/1942/27195

Fractal analysis of canard cycles with two breaking parameters and applications

Renato Huzak

Hasselt University, Campus Diepenbeek, Agoralaan Gebouw D, 3590 Diepenbeek, Belgium

Domagoj Vlah

University of Zagreb, Faculty of Electrical Engineering and Computing, Department of Applied Mathematics, Unska 3, 10000 Zagreb, Croatia

Abstract

In previous work [13] we introduced a new box dimension method for computation of the number of limit cycles in planar slow-fast systems, Hausdorff close to balanced canard cycles with one breaking mechanism (the Hopf breaking mechanism or the jump breaking mechanism). This geometric approach consists of a simple iteration method for finding one orbit of the so-called slow relation function and of the calculation of the box dimension of that orbit. Then we read the cyclicity of the balanced canard cycles from the box dimension. The purpose of the present paper is twofold. First, we generalize the box dimension method to canard cycles with two breaking mechanisms. Second, we apply the method from [13] and our generalized method to a number of interesting examples of canard cycles with one breaking mechanism and with two breaking mechanisms respectively.

1 Introduction

The (generic) *Hopf breaking mechanism* [7] is considered to be one of the most important mechanisms for generating limit cycles, Hausdorff close to so called *canard* cycles, in planar *slow-fast* systems (see also [1, 6, 9, 15]). A typical example of such generic Hopf breaking mechanisms is the following smooth slow-fast Liénard equation:

$$\left\{ \begin{array}{rcl} \dot{x} & = & y - \frac{1}{2}x^2 \\ \dot{y} & = & \epsilon\big(b_0 - x + x^2 H(x,\mu)\big), \end{array} \right. \tag{1}$$

where $\epsilon \geq 0$ is the singular perturbation parameter, b_0 is the breaking parameter, $\mu \in \mathbb{R}^m$, for some $m \geq 0$, and H is a smooth function (i.e., C^∞-smooth). We denote the (ϵ, b_0, μ)-family (1) by $L_{\epsilon,b_0,\mu}$. The *fast subsystem* $L_{0,b_0,\mu}$ of $L_{\epsilon,b_0,\mu}$

consists of fast regular horizontal orbits and a curve of singularities $\{y = \frac{1}{2}x^2\}$, called the *critical curve*. See Fig. 1. All singularities of the critical curve are normally hyperbolic, attracting when $x > 0$ and repelling when $x < 0$, except the origin where we deal with a *nilpotent contact* point. The dynamics of $L_{\epsilon,b_0,\mu}$, with $\epsilon > 0$ and $\epsilon \sim 0$, near the critical curve, away from the contact point, is given by the well known *slow dynamics* $x' = -1 + xH(x, \mu)$ (see e.g. [13]). Since the slow dynamics points from the attracting part to the repelling part of the critical curve near $x = 0$ (note that $x' < 0$ for $x \sim 0$), the following two questions arise naturally: *Under what conditions can $L_{\epsilon,b_0,\mu}$ have limit cycles close in the Hausdorff sense to the limit periodic set Γ_{y_0}, $y_0 > 0$, consisting of the fast horizontal orbit of $L_{0,b_0,\mu}$ through the point $(x, y) = (0, y_0)$ and the part of the critical curve between the points $(x, y) = (-\sqrt{2y_0}, y_0)$ and $(x, y) = (\sqrt{2y_0}, y_0)$? How do we obtain a sharp upper bound for the number of limit cycles which can bifurcate from Γ_{y_0}, for $(\epsilon, b_0, \mu) \sim (0, 0, \mu_0)$?* The limit periodic set Γ_{y_0} is often called a *slow-fast cycle* because it contains (fast) orbits of the fast subsystem and parts of the critical curve. Moreover, we can say that the slow-fast cycle Γ_{y_0} is *canard*, since it contains both attracting and repelling parts of the critical curve. We call limit cycles of $L_{\epsilon,b_0,\mu}$, Hausdorff close to slow-fast cycles, *relaxation oscillations*. See e.g. [10, 15].

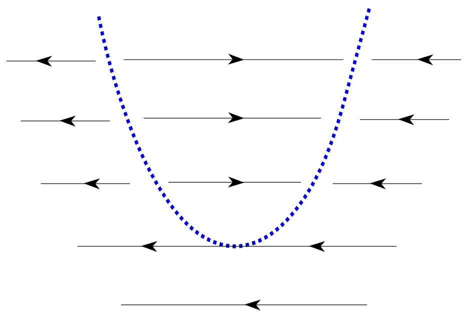

Figure 1: The fast subsystem $L_{0,b_0,\mu}$.

The above questions have been answered in [2, 7], in the case of regular slow dynamics, and in [3], in the presence of the slow dynamics with singularities (located away from the contact point). Let us focus on the regular slow dynamics (i.e., $-1 + xH(x, \mu_0) < 0$ for all $x \in [-\sqrt{2y_0}, \sqrt{2y_0}]$). Following [2, 7], a bound on the number of relaxation oscillations, Hausdorff close to Γ_{y_0}, can be obtained by studying zeros of the *slow divergence integral* along the critical curve $[-\sqrt{2y}, \sqrt{2y}]$:

$$I(y, \mu) := \int_{-\sqrt{2y}}^{\sqrt{2y}} \frac{\rho d\rho}{-1 + \rho H(\rho, \mu)}, \ (y, \mu) \sim (y_0, \mu_0). \tag{2}$$

(Note that the divergence of $L_{0,b_0,\mu}$ along the critical curve $\{y = \frac{1}{2}x^2\}$ is equal to $-x$.) The canard cycle Γ_{y_0} can generate at most (1+ the multiplicity of zero of $I(y, \mu_0)$ at $y = y_0$) limit cycles for $(\epsilon, b_0, \mu) \sim (0, 0, \mu_0)$.

A recently introduced method, called *box dimension method* (see [13]), provides a new tool for studying the cyclicity of Γ_{y_0} near $\mu = \mu_0$ in the family

$L_{\epsilon,b_0,\mu}$, *without computing directly the slow divergence integral* I. The box dimension method is based on the fractal analysis [11, 17] of the so called *slow relation function* and consists essentially of two steps (see Theorem 2 of [13]):

1. Choose any real number y_1, with $y_1 \sim y_0$ and $y_1 \neq y_0$, and generate the orbit $\mathcal{O} := \{y_1, y_2, y_3, \dots\}$ of y_1 by using the following recursive formula:

$$\int_{-\sqrt{2y_{n+1}}}^{\sqrt{2y_n}} \frac{\rho d\rho}{-1+\rho H(\rho,\mu_0)} = 0, \ n \geq 1.$$

   We suppose that $y_n \to y_0$ (under this assumption Γ_{y_0} is a *balanced* canard cycle at level $\mu = \mu_0$, i.e. $I(y_0, \mu_0) = 0$). For more details about the convergence of $(y_n)_{n\geq 1}$ see [13].

2. Compute the box dimension $\dim_B \mathcal{O} \in \{0, \frac{1}{2}, \frac{2}{3}, \frac{3}{4}, \dots\} \cup \{1\}$ of the orbit $\mathcal{O}$. If $\dim_B \mathcal{O} < 1$, then the cyclicity of Γ_{y_0} near $\mu = \mu_0$ is bounded by $\frac{2-\dim_B \mathcal{O}}{1-\dim_B \mathcal{O}}$. Roughly speaking, the box dimension measures the density of the orbit $\mathcal{O}$ near $y = y_0$; the bigger the box dimension of the orbit $\mathcal{O}$, the more relaxation oscillations can be created near Γ_{y_0}, for $(\epsilon, b_0, \mu) \sim (0, 0, \mu_0)$. For a precise definition of the box dimension see Section 2.

The reason for using the box dimension method is twofold. First, the method can be used when it is difficult to compute the slow divergence integral. We point out that the box dimension method has been developed in a more general framework of [13] (hence not only in the case of the Liénard system (1)), and therefore we can expect the slow divergence integral to be difficult from a computational point of view. Furthermore, *the box dimension of the orbit* $\mathcal{O}$ *is independent of the choice of the initial point* y_1. This is a simple consequence of (7) in Theorem 1 because $\mathcal{O}$ represents the orbit of y_1 generated by the (smooth) slow relation function that plays the role of the smooth function g in the statement of Theorem 1. (y_0 is a fixed point of the slow relation function; for more details we refer to [13].) Thus, it suffices to generate one orbit $\mathcal{O}$ and to compute $\dim_B \mathcal{O}$. *In Section 5, we apply the box dimension method to a number of polynomial Liénard equations of form (1) and we can easily obtain a sharp upper bound for the number of relaxation oscillations, Hausdorff close to* Γ_{y_0}, *by computing numerically the box dimension* $\dim_B \mathcal{O}$ *in Mathematica. To compute the box dimension, we use Tricot method [18] explained in the proof of Theorem 1.*

We point out that the notion of *Hausdorff dimension*, closely related to the notion of box dimension, is not suitable for the study of canard cycles due to its countable stability property (the Hausdorff dimension of $\mathcal{O}$ is trivial). See e.g. [12].

The principal purpose of the present paper is to generalize the box dimension method to canard cycles with two breaking parameters, studied in [10, 16], and to apply it to a number of polynomial Liénard (and non-Liénard) equations. See Fig. 2. For the sake of readability we have chosen to present the method in a special framework of smooth planar slow-fast systems of the following (Liénard) form:

$$X_{\epsilon,a_0,b_0,\mu} : \left\{ \begin{array}{rcl} \dot{x} &=& y - F(x, a_0, \mu) \\ \dot{y} &=& \epsilon G(x, b_0, \mu), \end{array} \right. \tag{3}$$

where F and G are smooth, $\epsilon \geq 0$ is a singular perturbation parameter, $(a_0, b_0) \sim (0,0)$ are two breaking parameters and μ is kept in a compact subset of $\mathbb{R}^m$, with $m \geq 0$. (When $m = 0$, we don't have the parameter μ.) A model similar to (3) has been used in [10] (with $m = 0$) and in [16] (with $m \geq 1$). Since the results obtained in [10, 16] are valid for a larger class of planar slow-fast systems, the fractal analysis [11, 17] can be applied not only to the Liénard model (3) but also to a broader class of planar slow-fast systems with two breaking parameters.

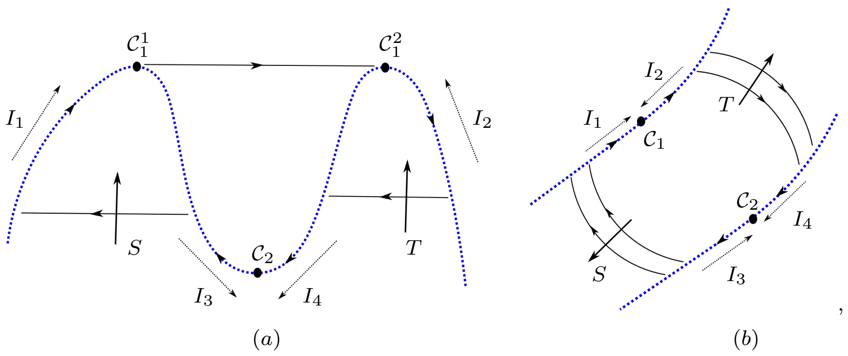

Figure 2: Canard cycles with two breaking parameters, at level $\epsilon = 0$. (a) One jump breaking mechanism, with two jump points $\mathcal{C}_1^1$ and $\mathcal{C}_1^2$, and one Hopf breaking mechanism with a turning point $\mathcal{C}_2$. (b) Two Hopf mechanisms with turning points $\mathcal{C}_1$ and $\mathcal{C}_2$.

Let $\mu_0 \in \mathbb{R}^m$ be fixed. Following [10, 16], if we want to observe limit cycles of $X_{\epsilon,a_0,b_0,\mu}$ $((\epsilon, a_0, b_0, \mu) \sim (0, 0, 0, \mu_0))$, in the Hausdorff sense close to canard cycles with two breaking mechanisms, the smooth functions F and G should meet the following conditions.

1. The functions F and G are well defined for $(a_0, b_0, \mu) \sim (0, 0, \mu_0)$ and for $x \in [-\tilde{x}, \tilde{x}]$, with $\tilde{x} > 0$.
2. (Jump mechanism) The function $F(x, a_0, \mu)$, $\mu \sim \mu_0$, has two maxima of Morse type at $x = x_1 = x_1(a_0, \mu)$ and $x = x_2 = x_2(a_0, \mu)$ $(-\tilde{x} < x_1 < 0 < x_2 < \tilde{x})$ such that $F(x_1(0, \mu), 0, \mu) - F(x_2(0, \mu), 0, \mu) = 0$, for all $\mu \sim \mu_0$. See Fig 2(a). We suppose that the point $\mathcal{C}_1^i = (x_i(0, \mu_0), F(x_i(0, \mu_0), 0, \mu_0))$ is a jump point for $i = 1, 2$ (i.e. $G(x_i(0, \mu_0), 0, \mu_0) \neq 0$ for $i = 1, 2$). Furthermore, we suppose that the parameter a_0 is a breaking parameter for the jump mechanism $(\mathcal{C}_1^1, \mathcal{C}_1^2)$ (i.e. $\frac{\partial}{\partial a_0}(F(x_1, a_0, \mu) - F(x_2, a_0, \mu)) \neq 0$ for $a_0 = 0$). This means that the connection between $\mathcal{C}_1^1$ and $\mathcal{C}_1^2$ becomes broken in a regular way as we vary $a_0 \sim 0$.
3. (Hopf mechanism) We suppose that $F(0, a_0, \mu) = 0$ and that $F(x, 0, \mu)$ has a minimum of Morse type at $x = 0$. Moreover, the point $\mathcal{C}_2 = (0, 0)$ is a (generic) turning point (i.e. $G(x, 0, \mu)$ has a simple zero at $x = 0$ for each $\mu \sim \mu_0$) and we assume that b_0 is a breaking parameter for the Hopf mechanism (i.e. $\frac{\partial G}{\partial b_0}(0, 0, \mu) \neq 0$).
4. (Regular slow dynamics) The critical curve $\{y = F(x, a_0, \mu)\}$ of $X_{0,a_0,b_0,\mu}$ is hyperbolically attracting when $x < x_1$ or $x \in]0, x_2[$ (i.e. $\frac{\partial F}{\partial x}(x, 0, \mu_0) >$

0, for $x \in [-\tilde{x}, x_1(0,\mu_0)[\cup]0, x_2(0,\mu_0)[)$ and hyperbolically repelling if $x \in]x_1, 0[$ or $x > x_2$ (i.e. $\frac{\partial F}{\partial x}(x,0,\mu_0) < 0$, for all $x \in]x_1(0,\mu_0), 0[\cup]x_2(0,\mu_0), \tilde{x}]$).

Now, we can define the slow dynamics of $X_{\epsilon,a_0,b_0,\mu}$ along the critical curve, away from the contact points $\mathcal{C}_1^{1,2}$ and $\mathcal{C}_2$:

$$x' = \frac{G(x,0,\mu)}{\frac{\partial F}{\partial x}(x,0,\mu)}.$$

We suppose that the slow dynamics is regular (i.e. $G(x,0,\mu) < 0$ for $x > 0$ and $G(x,0,\mu) > 0$ for $x < 0$).

A typical example of such a slow-fast system $X_{\epsilon,a_0,b_0,\mu}$ is $\{\dot{x} = y - (a_0 x + \frac{1}{2}x^2 - \frac{1}{4}x^4), \dot{y} = \epsilon(b_0 - x + O(x^2))\}$, for a suitably chosen function $O(x^2)$. For more details see [10, 16] and Section 5.

Under the above assumptions, we can detect a canard cycle in $X_{\epsilon,a_0,b_0,\mu}$, at level $(\epsilon, a_0, b_0, \mu) = (0,0,0,\mu_0)$. See Fig 2(a). First, we assume that vertical section S (resp. T) is parametrized by the y-coordinate denoted by z (resp. w). The canard cycle Γ_{z_0,w_0} consists of: (a) the fast orbit that cuts S at level $y = z_0$ (the α-limit set (resp. the ω-limit set) of that orbit is denoted by (x_1^α, z_0) (resp. (x_1^ω, z_0))); (b) the attracting part of the critical curve between (x_1^ω, z_0) and the jump point $\mathcal{C}_1^1$; (c) the fast orbit connecting $\mathcal{C}_1^1$ and $\mathcal{C}_1^2$; (d) the repelling part of the critical curve between $\mathcal{C}_1^2$ and the α-limit set of the fast orbit cutting T at level $y = w_0$, denoted by (x_2^α, w_0); (e) the fast orbit at level $y = w_0$, defined in (d); (f) the attracting part of the critical curve between the ω-limit set (x_2^ω, w_0) of the fast orbit from (e) and the turning point $\mathcal{C}_2$; (g) and the repelling part of the critical curve between $\mathcal{C}_2$ and (x_1^α, z_0).

To each part of the critical curve contained in Γ_{z_0,w_0} we attach a slow divergence integral defined near $(z, w, \mu) = (z_0, w_0, \mu_0)$ (see Fig 2(a)):

$$\begin{cases} I_1(z,\mu) := -\int_{x_1^\omega(z,\mu)}^{x_1(0,\mu)} \frac{(\frac{\partial F}{\partial x}(x,0,\mu))^2}{G(x,0,\mu)} dx, \ I_2(w,\mu) := -\int_{x_2^\alpha(w,\mu)}^{x_2(0,\mu)} \frac{(\frac{\partial F}{\partial x}(x,0,\mu))^2}{G(x,0,\mu)} dx \\ I_3(z,\mu) := -\int_{x_1^\alpha(z,\mu)}^{0} \frac{(\frac{\partial F}{\partial x}(x,0,\mu))^2}{G(x,0,\mu)} dx, \ I_4(w,\mu) := -\int_{x_2^\omega(w,\mu)}^{0} \frac{(\frac{\partial F}{\partial x}(x,0,\mu))^2}{G(x,0,\mu)} dx \end{cases} \tag{4}$$

Observe that Assumption 4 implies that $I_i < 0$, $i = 1,2,3,4$, and

$$\frac{\partial I_1}{\partial z}, \frac{\partial I_2}{\partial w} > 0, \quad \frac{\partial I_3}{\partial z}, \frac{\partial I_4}{\partial w} < 0. \tag{5}$$

One crucial assumption in [13] is that the canard cycle Γ_{y_0} in (1) is *balanced along one breaking mechanism.* In the present paper, we assume that the canard cycle Γ_{z_0,w_0} is *balanced along two breaking mechanisms*, at level $\mu = \mu_0$ (i.e. $I_1(z_0,\mu_0) - I_2(w_0,\mu_0) = 0$ and $I_3(z_0,\mu_0) - I_4(w_0,\mu_0) = 0$). A simple consequence of (5) is that there exist unique smooth functions $S_1(z,\mu)$ and $S_2(z,\mu)$ such that $w_0 = S_1(z_0,\mu_0) = S_2(z_0,\mu_0)$, $I_1(z,\mu) = I_2(S_1(z,\mu),\mu)$ and $I_3(z,\mu) = I_4(S_2(z,\mu),\mu)$ for all $(z,\mu) \sim (z_0,\mu_0)$. We call S_1 and S_2 *slow relation functions* (see e.g. [7]).

The main goal of our paper is to prove the following box-dimension method for finding out how many limit cycles of $X_{\epsilon,a_0,b_0,\mu}$ can be born for $(\epsilon, a_0, b_0, \mu) \sim (0,0,0,\mu_0)$, Hausdorff close to the balanced canard cycle Γ_{z_0,w_0} (see Theorem 2).

1. Take any real number z_1, with $z_1 \sim z_0$ and $z_1 > z_0$, and generate the orbit $\tilde{\mathcal{O}} := \{z_1, z_2, z_3, \dots\}$ of z_1 by using the following recursive formula:

   $$z_{n+1} = z_n - (w_n^2 - w_n^1),\ n \geq 1,$$

   where $w_n^1 \sim w_0$ and $w_n^2 \sim w_0$ are unique numbers with the property $I_1(z_n, \mu_0) = I_2(w_n^1, \mu_0)$ and $I_3(z_n, \mu_0) = I_4(w_n^2, \mu_0)$. In other words, one has $w_n^i = S_i(z_n, \mu_0)$ for $i = 1, 2$.

2. Compute the box dimension $\dim_B \tilde{\mathcal{O}} \in \{0, \frac{1}{2}, \frac{2}{3}, \frac{3}{4}, \dots\} \cup \{1\}$. If $\dim_B \tilde{\mathcal{O}} < 1$, then Γ_{z_0,w_0} can produce at most $\frac{3-2\dim_B \tilde{\mathcal{O}}}{1-\dim_B \tilde{\mathcal{O}}}$ limit cycles, for $(\epsilon, a_0, b_0, \mu) \sim (0, 0, 0, \mu_0)$ (we break both mechanisms (a_0, b_0)).

This algorithm works under the assumption that the function $z \to S_2(z, \mu_0) - S_1(z, \mu_0)$ fulfils the following conditions of Theorem 1 on $[z_0, z_0 + \eta[$, with $\eta \sim 0$ and $\eta > 0$: $S_2 - S_1$, with $\mu = \mu_0$, is a smooth function on $[z_0, z_0 + \eta[$, positive and nondecreasing on $]z_0, z_0 + \eta[$, $S_2(z_0, \mu_0) - S_1(z_0, \mu_0) = 0$ and $S_2(z, \mu_0) - S_1(z, \mu_0) < z - z_0$, for each $z \in]z_0, z_0 + \eta[$. Under this assumption, the sequence $(z_n)_{n\geq 1}$ (resp. $(z_n - z_{n+1})_{n\geq 1}$) tends monotonically to z_0 (resp. 0) and therefore we can use the Tricot method to compute $\dim_B \tilde{\mathcal{O}}$ (see the proof of Theorem 1). Note that $\tilde{\mathcal{O}}$ is the orbit of $z_1 \in]z_0, z_0 + \eta[$ by the function $\mathrm{id} - (S_2 - S_1)$, for $\mu = \mu_0$.

Let $k \geq 1$ be the multiplicity of z_0 of the function $S_2 - S_1$, with $\mu = \mu_0$. We point out that the above assumption is not restrictive, since either the function $S_2 - S_1$ or the function $S_1 - S_2$ fulfils the conditions of Theorem 1, at least when $1 < k < \infty$. When $k = 1$, the derivative of $S_2 - S_1$ is nonzero, for $(z, \mu) = (z_0, \mu_0)$:

$$\frac{\partial(S_2 - S_1)}{\partial z}(z_0, \mu_0) = \frac{\frac{\partial I_2}{\partial w}(w_0, \mu_0)\frac{\partial I_3}{\partial z}(z_0, \mu_0) - \frac{\partial I_4}{\partial w}(w_0, \mu_0)\frac{\partial I_1}{\partial z}(z_0, \mu_0)}{\frac{\partial I_2}{\partial w}(w_0, \mu_0)\frac{\partial I_4}{\partial w}(w_0, \mu_0)}. \tag{6}$$

In this case, we call Γ_{z_0,w_0} a *generic balanced canard cycle* (see e.g. [10, 7]). When (6) is between -1 and 1, the function $S_2 - S_1$ (or $S_1 - S_2$) fulfils the conditions of Theorem 1. If $k = \infty$, then $\dim_B \tilde{\mathcal{O}} = 1$ (see Theorem 1).

Like in [13], the box dimension $\dim_B \tilde{\mathcal{O}}$ is independent of the initial point z_1. Thus, if we want to find the cyclicity of Γ_{z_0,w_0} near $\mu = \mu_0$, it suffices to compute the box dimension of one orbit that we generate by using the equations $\{I_1(z, \mu_0) = I_2(w, \mu_0)\}$ and $\{I_3(z, \mu_0) = I_4(w, \mu_0)\}$.

In Section 2 we define the box dimension and recall the fractal analysis [11, 17] in one-dimensional ambient space. In Section 3 we state our main results. The cyclicity results for Γ_{z_0,w_0} are obtained in terms of the box dimension and they depend on how many breaking parameter mechanisms we break. We prove our main results in Section 4. In Section 5 we apply our box dimension methods to (balanced) canard cycles with one or two breaking parameters. We find the box dimension of the canard cycles using Mathematica.

2 Minkowski content and box dimension of bounded sets

First we recall the notions of Minkowski content and box dimension of a bounded set in $\mathbb{R}^n$. For more details, we refer the interested reader to [12, 14, 18].

We denote by U_δ the δ-neighborhood of a bounded set $U \subset \mathbb{R}^n$ ($U_\delta = \{x \in \mathbb{R}^n \mid d(x, U) \leq \delta\}$). Let $|U_\delta|$ be the Lebesgue measure of U_δ. The density of accumulation of the set U in $\mathbb{R}^n$ is closely related to the rate at which $|U_\delta|$ decreases when $\delta \to 0$, and it is typically measured by the box dimension and the Minkowski content of U. *The lower s-dimensional Minkowski content of U* (resp. *the upper s-dimensional Minkowski content of U*), $0 \leq s \leq n$, is defined by

$$\mathcal{M}_*^s(U) = \liminf_{\delta \to 0} \frac{|U_\delta|}{\delta^{n-s}} \quad \left(\text{resp. } \mathcal{M}^{*s}(U) = \limsup_{\delta \to 0} \frac{|U_\delta|}{\delta^{n-s}}\right).$$

The lower box dimension of U (resp. *the upper box dimension of U*) is now defined as follows:

$$\underline{\dim}_B U = \inf\{s \geq 0 \mid \mathcal{M}_*^s(U) = 0\} \ \left(\text{resp. } \overline{\dim}_B U = \inf\{s \geq 0 \mid \mathcal{M}^{*s}(U) = 0\}\right).$$

If $\underline{\dim}_B U = \overline{\dim}_B U$, then we denote it by $\dim_B U$. We call $\dim_B U$ the *box dimension of U*. We refer the reader to [12] for properties of Minkowski content and box dimension. In the rest of this section we focus on one-dimensional ambient space ($n = 1$) and recall an interesting result of [11, 17] establishing the bijective correspondence between the multiplicity of an isolated fixed point of a smooth function and the box dimension of any orbit of the function accumulating at the fixed point. The box dimension of the orbits near a hyperbolic fixed point is equal to 0 and the box dimension of the orbits near nonhyperbolic fixed point is positive (see Theorem 1).

Suppose that f is a smooth nondecreasing function on $[0, \eta[$, with $\eta \sim 0$ and $\eta > 0$, $f(0) = 0$ and $0 < f(x) < x$, for each $x \in]0, \eta[$. We define

$$g(x) := x - f(x)$$

and $\mathcal{O}_{x_0}^g := \{x_n = g^n(x_0) \mid n \in \mathbb{N}\}$, where $x_0 \in]0, \eta[$. $\mathcal{O}_{x_0}^g$ represents the orbit of x_0 by g and it tends monotonically to zero, the fixed point of g. Since the box dimension $\dim_B \mathcal{O}_{x_0}^g$ is independent of the initial point x_0 (see [11] or Theorem 1), we can define *the box dimension of g*: $\dim_B g := \dim_B \mathcal{O}_{x_0}^g$, for any $x_0 \in]0, \eta[$.

The multiplicity of the fixed point 0 of the smooth function g is equal to k if $x = 0$ is a zero of multiplicity k of f, i.e. $f(0) = \cdots = f^{(k-1)}(0) = 0$ and $f^{(k)}(0) \neq 0$. We write $m_0^{fix}(g) = k$. Furthermore, the multiplicity of the fixed point 0 of g is ∞ if $f^{(k)}(0) = 0$, for each $k \in \mathbb{N}$.

Suppose that $f_1(x)$ and $f_2(x)$ are two positive functions defined for $x > 0$ and $x \sim 0$. Then we write $f_1(x) \simeq f_2(x)$ as $x \to 0$ if $Af_2(x) \leq f_1(x) \leq Bf_2(x)$, where A and B are two positive constants, $x > 0$ and $x \sim 0$.

Theorem 1 ([11, 17])**.** *Let f be a smooth function on $[0, \eta[$, positive and nondecreasing on $]0, \eta[$ and $f(0) = 0$. Put $U = \mathcal{O}_{x_0}^g$, with $g = id - f$ and $x_0 \in [0, \eta[$.*

If $1 < m_0^{fix}(g) < \infty$ (i.e. g has a nonhyperbolic fixed point at 0), then

$$|U_\delta| \simeq \delta^{\frac{1}{m_0^{fix}(g)}}, \ \textit{as } \delta \to 0.$$

If $m_0^{fix}(g) = 1$ and $f(x) < x$ on $]0, \eta[$ (i.e. g has a hyperbolic fixed point at 0), then

$$|U_\delta| \simeq \begin{cases} \delta(-\log\delta), & f'(0) < 1 \textit{(the "standard" hyperbolic case)}, \\ \delta\log(-\log\delta), & f'(0) = 1 \textit{(the "degenerate" hyperbolic case)}, \end{cases} \quad \textit{as } \delta \to 0.$$

For $1 \le m_0^{fix}(g) < \infty$, a bijective correspondence holds

$$m_0^{fix}(g) = \frac{1}{1 - \dim_B g}. \tag{7}$$

If $m_0^{fix}(g) = \infty$, then $\dim_B g = 1$.

Proof. The proof of Theorem 1 can be found in [11] or [17]. The proof has been given in [13] in two special cases: 1. $f(x) = x - x^2$ (the hyperbolic case), 2. $f(x) = x^2$ (the nonhyperbolic case). For the sake of completeness we repeat it here.

In both cases, for every $\delta \sim 0$ and $\delta > 0$, we decompose the δ-neighborhood U_δ of $U = \mathcal{O}_{x_0}^g$ into two parts, the nucleus N_δ and the tail T_δ (see Fig. 3). This method of estimating the length of the δ-neighborhood as $\delta \to 0$ by decomposing it into tail and nucleus is taken from [18]. The tail T_δ is the union of δ-neighborhoods of the points $x_0, x_1, \ldots, x_{n_\delta - 1}$. The index $n_\delta \in \mathbb{N}$ is the smallest index such that the δ-neighborhood of x_{n_δ} and the δ-neighborhood of $x_{n_\delta+1}$ have non-empty intersection. The index n_δ is well-defined, and the δ-neighborhood of x_n and the δ-neighborhood of x_{n+1} have non-empty intersection for each $n \ge n_\delta$, because the sequence $(x_n - x_{n+1})_{n\in\mathbb{N}} = (f(x_n))_{n\in\mathbb{N}}$ tends monotonically to zero. Thus, we have $|U_\delta| = |T_\delta| + |N_\delta|$, $|T_\delta| = n_\delta 2\delta \simeq n_\delta \delta$, as $\delta \to 0$, and $|N_\delta| = x_{n_\delta} + 2\delta$.

1. $f(x) = x - x^2$. Thus $g(x) = x^2$, $m_0^{fix}(g) = 1$ and $f'(0) = 1$. Moreover, we have $x_n = g(x_{n-1}) = x_0^{2^n}$, $n \ge 0$.

To estimate n_δ and x_{n_δ} as $\delta \to 0$, we use $2\delta \simeq (x_{n_\delta} - x_{n_\delta+1}) = f(x_{n_\delta}) = x_{n_\delta} - x_{n_\delta}^2 \simeq x_{n_\delta} = x_0^{2^{n_\delta}}$, as $\delta \to 0$. This implies that $n_\delta \simeq \log(-\log\delta)$ and $x_{n_\delta} \simeq \delta$, as $\delta \to 0$. Thus, we obtain

$$|T_\delta| \simeq \delta\log(-\log\delta),\ |N_\delta| \simeq \delta,\ \delta \to 0.$$

Now it can be easily seen that $|U_\delta| \simeq \delta\log(-\log\delta)$, as $\delta \to 0$, and $\dim_B g = 0$. Note that the estimates above and the box dimension do not depend on the choice of the initial point x_0 of the orbit.

2. $f(x) = x^2$. Then $g(x) = x - x^2$ and $m_0^{fix}(g) = 2$. That is, $f'(0) = 0$, $f''(0) > 0$. First, by solving formally the difference equation $x_{n+1} = g(x_n) = x_n - x_n^2$, we estimate the asymptotic behavior $x_n \simeq n^{-1}$, $n \to \infty$. To estimate the asymptotic behavior of n_δ, as $\delta \to 0$, we use, as above, the relation $2\delta \simeq (x_{n_\delta} - x_{n_{\delta+1}})$. Since $x_n - x_{n+1} = f(x_n) = x_n^2 \simeq n^{-2}$, we get that $n_\delta \simeq \delta^{-1/2}$, as $\delta \to 0$. Consequently, $x_{n_\delta} \simeq \delta^{1/2}$. we now have

$$|T_\delta| = 2\delta n_\delta \simeq \delta^{1/2},\ |N_\delta| = x_{n_\delta} + 2\delta \simeq \delta^{1/2},\ \delta \to 0.$$

Therefore, $|U_\delta| \simeq \delta^{1/2}$, $\delta \to 0$, and $\dim_B g = \frac{1}{2}$. All calculations are independent of the initial point x_0. ☐

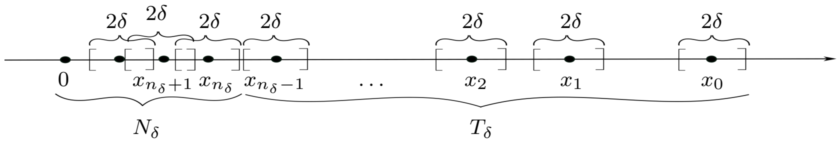

Figure 3: U_δ has two parts: the nucleus N_δ, and the tail T_δ. The tail T_δ contains all (2δ)-intervals of U_δ before they start to overlap at the point x_{n_δ}.

Remark 1. *It follows from (7) that* $\dim_B g$ *is trivial, if* g *has a hyperbolic fixed point at* 0 *(the orbit* $\mathcal{O}^g_{x_0}$ *tends exponentially fast to* 0*), or positive (*$\dim_B g \in \{\frac{1}{2}, \frac{2}{3}, \frac{3}{4}, \dots\} \cup \{1\}$*), if* g *has a nonhyperbolic fixed point at the origin. Note that the box dimension is trivial in both standard and degenerate hyperbolic case, though* $\mathcal{O}^g_{x_0}$ *in the degenerate hyperbolic case tends to* 0 *faster than* $\mathcal{O}^g_{x_0}$ *in the standard hyperbolic case. See e.g. [17] for more details.*

3 Statement of the results

In this section we consider a smooth slow-fast Liénard system $X_{\epsilon,a_0,b_0,\mu}$, given in (3), and state our main results under Assumptions 1–4 of Section 1. *The cyclicity of a canard cycle* Γ_{z_0,w_0} *in the family* $X_{\epsilon,a_0,b_0,\mu}$ is bounded from above by $M \in \mathbb{N}$ if we can find $\epsilon_0 > 0$, a Hausdorff neighborhood $\mathcal{V}$ of Γ_{z_0,w_0} and a neighborhood $\mathcal{W}$ of $(0, 0, \mu_0)$ in (a_0, b_0, μ)-space such that $X_{\epsilon,a_0,b_0,\mu}$ generates at most M limit cycles inside $\mathcal{V}$, for all $(\epsilon, a_0, b_0, \mu) \in [0, \epsilon_0] \times \mathcal{W}$. (We call the smallest M with this property the cyclicity of Γ_{z_0,w_0} in the family $X_{\epsilon,a_0,b_0,\mu}$.)

Following [10, 7, 16], we distinguish between 3 different types of "creation" of limit cycles near Γ_{z_0,w_0}: (a) we break both mechanisms (see Assumptions 2 and 3 of Section 1); (b) we break precisely one of the two mechanisms; (c) both mechanisms remain unbroken. If we break both mechanisms in $X_{\epsilon,a_0,b_0,\mu}$, we obtain a sharp upper bound for the cyclicity of Γ_{z_0,w_0} in the family $X_{\epsilon,a_0,b_0,\mu}$.

Theorem 2. *Let* $X_{\epsilon,a_0,b_0,\mu}$ *be defined in (3) and suppose that* Γ_{z_0,w_0} *is a balanced canard cycle for* $\mu = \mu_0$*. Furthermore, suppose that the smooth function* $f(z) = S_2(z, \mu_0) - S_1(z, \mu_0)$*, defined in Section 1, satisfies the conditions of Theorem 1 on* $[z_0, z_0 + \eta[$*, with* $\eta > 0$ *and* $\eta \sim 0$*. Let* $\mathcal{O}^g_{z_1}$ *be the orbit of* $z_1 \in]z_0, z_0 + \eta[$ *by* $g = id - f$*. Then* $\dim_B \mathcal{O}^g_{z_1}$ *is independent of the initial point* z_1 *and, if* $\dim_B \mathcal{O}^g_{z_1} < 1$*, the cyclicity of* Γ_{z_0,w_0} *in the family* $X_{\epsilon,a_0,b_0,\mu}$ *is bounded by* $\frac{3-2\dim_B \mathcal{O}^g_{z_1}}{1-\dim_B \mathcal{O}^g_{z_1}}$.

As we will see in Section 4.1, Theorem 2 is a direct consequence of Corollary 6 in [16] and Theorem 1.

Remark 2. *The box dimension method for canard cycles with two breaking parameters, introduced in Section 1, follows from Theorem 2.*

When at least one of the two breaking mechanisms remains unbroken, our model $X_{\epsilon,a_0,b_0,\mu}$ fits into the framework of [7], and we can easily study the number of limit cycles near Γ_{z_0,w_0} by using the same box dimension method. The only difference with the box dimension method based on Theorem 2 lies in the number of limit cycles near Γ_{z_0,w_0}: if precisely one of the two mechanisms remains unbroken (resp. both mechanisms remain unbroken), it decreases by one (resp. two) the upper bound.

Theorem 3. *Suppose that Γ_{z_0,w_0} is a balanced canard cycle for $\mu = \mu_0$ in the family $X_{\epsilon,a_0,b_0,\mu}$, and suppose that the smooth function $f(z) = S_2(z,\mu_0) - S_1(z,\mu_0)$ satisfies the conditions of Theorem 1 on $[z_0, z_0+\eta[$, with $\eta > 0$ and $\eta \sim 0$. Let $\mathcal{O}^g_{z_1}$ be the orbit of $z_1 \in]z_0, z_0+\eta[$ by $g = id - f$. Then $\dim_B \mathcal{O}^g_{z_1}$ is independent of the initial point z_1 and the following statements are true:*

1. ***(one mechanism remains unbroken)** If $\dim_B \mathcal{O}^g_{z_1} < 1$, then there exist smooth functions $a_0 = \mathcal{A}_0(\epsilon, \bar{b}_0, \mu) \sim 0$ and $\bar{b}_0 = \bar{\mathcal{B}}_0(\epsilon, a_0, \mu) \sim 0$ ($\bar{b}_0 := \frac{b_0}{\sqrt{\epsilon}}$) such that the systems $X_{\epsilon,\mathcal{A}_0(\epsilon,\bar{b}_0,\mu),\sqrt{\epsilon}\bar{b}_0,\mu}$ and $X_{\epsilon,a_0,\sqrt{\epsilon}\bar{\mathcal{B}}_0(\epsilon,a_0,\mu),\mu}$ contain at most $\frac{2-\dim_B \mathcal{O}^g_{z_1}}{1-\dim_B \mathcal{O}^g_{z_1}}$ limit cycles Hausdorff close to Γ_{z_0,w_0}, for each $(\epsilon, a_0, \bar{b}_0, \mu) \sim (0,0,0,\mu_0)$ and $\epsilon > 0$.*

2. ***(both mechanisms remain unbroken)** If $\dim_B \mathcal{O}^g_{z_1} < 1$, then there exist smooth functions $a_0 = \mathcal{A}_0(\epsilon,\mu) \sim 0$ and $\bar{b}_0 = \bar{\mathcal{B}}_0(\epsilon,\mu) \sim 0$ such that $X_{\epsilon,\mathcal{A}_0(\epsilon,\mu),\sqrt{\epsilon}\bar{\mathcal{B}}_0(\epsilon,\mu),\mu}$ contains at most $\frac{1}{1-\dim_B \mathcal{O}^g_{z_1}}$ limit cycles Hausdorff close to Γ_{z_0,w_0}, for each $(\epsilon,\mu) \sim (0,\mu_0)$ and $\epsilon > 0$.*

Theorem 3 will be proved in Section 4.2.

In the rest of this section, we focus on the case where the box dimension is trivial (i.e. $\dim_B \tilde{\mathcal{O}} = 0$). As we know from [13], the trivial box dimension $\dim_B \mathcal{O}$ in (1) leads to a saddle-node bifurcation of limit cycles when we vary the breaking parameter $b_0 \sim 0$ in (1) (see Theorem 3 of [13]). If we deal with canard cycles with two breaking mechanisms, then the trivial box dimension gives rise to a *cusp-catastrophy of limit cycles.*

Theorem 4. *Let Γ_{z_0,w_0} be a balanced canard cycle for $\mu = \mu_0$ in the family $X_{\epsilon,a_0,b_0,\mu}$. Suppose the smooth function $f(z) = S_2(z,\mu_0) - S_1(z,\mu_0)$ satisfies the conditions of Theorem 1 on $[z_0, z_0+\eta[$, with $\eta > 0$ and $\eta \sim 0$. If $\mathcal{O}^g_{z_1}$ is the orbit of $z_1 \in]z_0, z_0+\eta[$ by $g = id - f$ and if $\dim_B \mathcal{O}^g_{z_1} = 0$, then a limit cycle of codimension 2 bifurcates from Γ_{z_0,w_0} generically unfolded by the parameter $(a_0, b_0) \sim (0,0)$, for $\epsilon > 0$ small enough. The cyclicity of Γ_{z_0,w_0} in the family $X_{\epsilon,a_0,b_0,\mu}$ is equal to 3.*

Theorem 4 follows from Theorem 1 and [10] (see Section 4.3). We will apply Theorem 4 to the following slow-fast Liénard system:

$$\left\{ \begin{array}{rcl} \dot{x} & = & y - (a_0 x + \frac{1}{2}x^2 - \frac{1}{4}x^4) \\ \dot{y} & = & \epsilon\big(b_0 - x - 0.05(x^2 - x^4 + x^6 - 0.5x^8)\big), \end{array} \right.$$

with $(\epsilon, a_0, b_0) \sim (0,0,0)$, and we will detect 3 hyperbolic limit cycles near a suitably chosen balanced canard cycle. It will be proved numerically that the box dimension of one orbit $\tilde{\mathcal{O}}$, obtained by using the box dimension algorithm introduced in Section 1, is equal to 0 (see Section 5).

When the breaking parameter b_0 in (1) remains unbroken, then the system (1) has a unique (hyperbolic) limit cycle (Hausdorff) close to the balanced canard cycle Γ_{y_0} if $\dim_B \mathcal{O} = 0$ (for more details see Theorem 3 of [13]). Thus, if we have k balanced canard cycles $\Gamma_{y_0^1}, \ldots, \Gamma_{y_0^k}$, at which $\dim_B \mathcal{O} = 0$, then (1) has at least k hyperbolic limit cycles, for $\epsilon > 0$ small enough and b_0 unbroken. We obtain similar results when canard cycles have two breaking parameters.

Theorem 5. *Suppose that Γ_{z_0,w_0} is a balanced canard cycle for $\mu = \mu_0$ in the family $X_{\epsilon,a_0,b_0,\mu}$, and suppose that the smooth function $f(z) = S_2(z,\mu_0) - S_1(z,\mu_0)$ satisfies the conditions of Theorem 1 on $[z_0, z_0+\eta[$, with $\eta > 0$ and $\eta \sim 0$. Let $\mathcal{O}^g_{z_1}$ be the orbit of $z_1 \in]z_0, z_0+\eta[$ by $g = id - f$. If $\dim_B \mathcal{O}^g_{z_1} = 0$, then the following statements are true:*

1. *(**one mechanism remains unbroken**) There exist smooth functions $a_0 = \mathcal{A}_0(\epsilon, \bar{b}_0, \mu) \sim 0$ and $\bar{b}_0 = \bar{\mathcal{B}}_0(\epsilon, a_0, \mu) \sim 0$ ($\bar{b}_0 := \frac{b_0}{\sqrt{\epsilon}}$) such that the systems $X_{\epsilon,\mathcal{A}_0(\epsilon,\bar{b}_0,\mu),\sqrt{\epsilon}\bar{b}_0,\mu}$ and $X_{\epsilon,a_0,\sqrt{\epsilon}\bar{\mathcal{B}}_0(\epsilon,a_0,\mu),\mu}$ with fixed $\mu \sim \mu_0$, $\epsilon > 0$ and $\epsilon \sim 0$ contain a saddle-node bifurcation of limit cycles (Hausdorff) close to Γ_{z_0,w_0}.*
2. *(**both mechanisms remain unbroken**) There exist smooth functions $a_0 = \mathcal{A}_0(\epsilon,\mu) \sim 0$ and $\bar{b}_0 = \bar{\mathcal{B}}_0(\epsilon,\mu) \sim 0$ such that $X_{\epsilon,\mathcal{A}_0(\epsilon,\mu),\sqrt{\epsilon}\bar{\mathcal{B}}_0(\epsilon,\mu),\mu}$ with fixed $\mu \sim \mu_0$, $\epsilon > 0$ and $\epsilon \sim 0$ has a unique limit cycle that is hyperbolic and (Hausdorff) close to Γ_{z_0,w_0}.*

Theorem 5 follows from Theorem 1 and [7] (see Section 4.4). Theorem 5.2 can be useful when we want to construct slow-fast (Liénard) systems with more limit cycles than one would expect (see e.g. [8, 4, 5]). When we do not break the parameter (a_0, b_0), each balanced canard cycle Γ_{z_0,w_0} with the trivial box dimension generates one hyperbolic limit cycle.

4 Proofs of Theorem 2–Theorem 5

The results stated in Section 3 can be easily proved by combining Theorem 1 and the results of [10, 7, 16]. In this section we give a sketch of the proof of Theorem 2–Theorem 5. As mentioned in Section 1, the cyclicity results from Section 3 enable us to develop an efficient algorithm for the study of limit cycles that on one hand works with a minimum amount of information (we need only one orbit of the function $z \to z - (S_2(z,\mu_0) - S_1(z,\mu_0))$ but on the other hand uses a recently developed "geometric" approach from the fractal analysis (we compute the box dimension of the orbit). See Section 5.

4.1 Proof of Theorem 2

Since Γ_{z_0,w_0} is a balanced canard cycle of (3) for $\mu = \mu_0$, we have $S_2(z_0,\mu_0) - S_1(z_0,\mu_0) = w_0 - w_0 = 0$. We also have by definition of S_1 and S_2 that $I_1(z,\mu) = I_2(S_1(z,\mu),\mu)$ and $I_3(z,\mu) = I_4(S_2(z,\mu),\mu)$ for each $(z,\mu) \sim (z_0,\mu_0)$.

Suppose that the smooth function $f(z) := S_2(z,\mu_0) - S_1(z,\mu_0)$ satisfies the following conditions of Theorem 1 on $[z_0, z_0+\mu[$, with $\mu > 0$ and $\mu \sim 0$: $f(z_0) = 0$ (this is true because Γ_{z_0,w_0} is balanced), f is positive and nondecreasing on $]z_0, z_0+\mu[$, and $f(z) < z - z_0$ for all $z \in]z_0, z_0+\mu[$. If we denote by $\mathcal{O}^g_{z_1}$ the orbit of $z_1 \in]z_0, z_0+\eta[$ by $g = id - f$ and if $\dim_B \mathcal{O}^g_{z_1} < 1$, then the function f has a zero of multiplicity $l := \frac{1}{1-\dim_B \mathcal{O}^g_{z_1}} = \frac{1}{1-\dim_B g} < +\infty$ at $z = z_0$ (see (7)). In [16], this number l is called the intersection multiplicity of the curves $\{I_1(z,\mu_0) - I_2(w,\mu_0) = 0\}$ and $\{I_3(z,\mu_0) - I_4(w,\mu_0) = 0\}$ at the point (z_0,w_0). The following theorem plays a crucial role in the proof of Theorem 2 (see Corollary 6 of [16]):

Theorem 6. *Let's suppose that the curves* $\{I_1(z,\mu_0) - I_2(w,\mu_0) = 0\}$ *and* $\{I_3(z,\mu_0) - I_4(w,\mu_0) = 0\}$ *have an intersection multiplicity* $l < +\infty$ *at the point* $(z,w) = (z_0,w_0)$. *Then the cyclicity of* Γ_{z_0,w_0} *in the family (3) is bounded by* $l+2$.

Since $l = \frac{1}{1-\dim_B \mathcal{O}^g_{z_1}}$, Theorem 6 implies that the cyclicity of Γ_{z_0,w_0} in the family (3) is bounded by $\frac{3-2\dim_B \mathcal{O}^g_{z_1}}{1-\dim_B \mathcal{O}^g_{z_1}}$.

4.2 Proof of Theorem 3

Let conditions of Theorem 3 be satisfied. Following Theorem 1, the function f has a zero of multiplicity $l = \frac{1}{1-\dim_B \mathcal{O}^g_{z_1}} < +\infty$ at $z = z_0$. See also Section 4.1. Theorem 3.1 (resp. Theorem 3.2) follows now from Theorem 5.2(2) (resp. Theorem 5.2(1)) of [7]. Theorem 5.2(2) of [7] (resp. Theorem 5.2(1) of [7]) implies that Γ_{z_0,w_0} generates at most $l+1$ limit cycles (resp. at most l limit cycles) if we break one of the two mechanisms (resp. both mechanisms remain unbroken).

4.3 Proof of Theorem 4

Let conditions of Theorem 4 be satisfied. Following Theorem 1, the multiplicity of f is equal to 1 at the point $z = z_0$ because $\dim_B \mathcal{O}^g_{z_1} = 0$. From this together with (6) it follows that

$$\frac{\partial I_2}{\partial w}(w_0,\mu_0)\frac{\partial I_3}{\partial z}(z_0,\mu_0) - \frac{\partial I_4}{\partial w}(w_0,\mu_0)\frac{\partial I_1}{\partial z}(z_0,\mu_0) \neq 0.$$

We can define the total slow divergence integral of Γ_{z_0,w_0} as follows (see [10]):

$$I_T(z,w,\mu) := I_1(z,\mu) - I_2(w,\mu) + I_4(w,\mu) - I_3(z,\mu),\ (z,w,\mu) \sim (z_0,w_0,\mu_0).$$

The following theorem has been proved in [10] (Theorem 1.1):

Theorem 7. *Suppose that* $I_T(z_0,w_0,\mu_0) = 0$, $I_1(z_0,\mu_0) - I_2(w_0,\mu_0) = 0$ *and* $\frac{\partial I_2}{\partial w}(w_0,\mu_0)\frac{\partial I_3}{\partial z}(z_0,\mu_0) - \frac{\partial I_4}{\partial w}(w_0,\mu_0)\frac{\partial I_1}{\partial z}(z_0,\mu_0) \neq 0$. *Then a codimension* 2 *relaxation oscillation bifurcates from* Γ_{z_0,w_0}, *for* $\epsilon > 0$ *small enough and* $\mu \sim \mu_0$. *This degenerate limit cycle is generically unfolded by the breaking parameter* $(a_0,b_0) \sim (0,0)$, *for* $\epsilon > 0$ *small enough and* $\mu \sim \mu_0$, *producing systems having* 3 *hyperbolic limit cycles (Hausdorff) close to* Γ_{z_0,w_0}.

Now it suffices to notice that the condition $\{I_T(z_0,w_0,\mu_0) = I_1(z_0,\mu_0) - I_2(w_0,\mu_0) = 0\}$ is equivalent to $\{I_1(z_0,\mu_0) - I_2(w_0,\mu_0) = I_3(z_0,\mu_0) - I_4(w_0,\mu_0) = 0\}$.

4.4 Proof of Theorem 5

Let conditions of Theorem 5 be satisfied. Since $\dim_B \mathcal{O}^g_{z_1} = 0$, Theorem 1 implies that the function f has a zero of multiplicity 1 at $z = z_0$. Theorem 5.1 (resp. Theorem 5.2) follows now from Theorem 5.1(3) (resp. Theorem 5.1(2)) of [7]. Indeed, if f has a simple zero at $z = z_0$ and if we break exactly one breaking parameter, then for each $\mu \sim \mu_0$, $\epsilon \sim 0$ and $\epsilon > 0$ (3) contains a saddle-node bifurcation of limit cycles (Hausdorff) close to Γ_{z_0,w_0}, as we vary the broken parameter (see Theorem 5.1(3) of [7]). On the other hand, if f has a simple zero at $z = z_0$ and if both mechanisms remain unbroken, then Γ_{z_0,w_0} generates exactly one (hyperbolic) limit cycle (see Theorem 5.1(2) of [7]).

5 Applications

In this section we apply the box dimension method for balanced canard cycles with one breaking parameter (see Sections 5.3 and 5.4) and the box dimension method for balanced canard cycles with two breaking parameters (see Section 5.5) to slow-fast (polynomial) Liénard equations. We generate for each example several orbits of the balanced canard cycles, and we compute the box dimension of that orbits. We use Wolfram Mathematica.

We choose such Liénard equations for which we can find exact values of the box dimension such that we can compare it with our numerical estimates. Indeed, we can find the multiplicity of y_0 of the slow divergence integral (2) or the intersection multiplicity of the curves $\{I_1(z, \mu_0) - I_2(w, \mu_0) = 0\}$ and $\{I_3(z, \mu_0) - I_4(w, \mu_0) = 0\}$ at the point (z_0, w_0), and obtain the box dimension from (7).

5.1 Numerical computation of the box dimension

For a given system (1), which is chosen by prescribing parameter μ_0, we first compute numerically a zero y_0 of the slow divergence integral (2). In the case of a system (3), having canard cycles with two breaking parameters, we numerically compute z_0 and w_0 such that slow divergence integrals (4) satisfy $I_1(z_0, \mu_0) - I_2(w_0, \mu_0) = 0$ and $I_3(z_0, \mu_0) - I_4(w_0, \mu_0) = 0$.

For each example system (11), (12) and (13), we numerically compute five different orbits $\mathcal{O}^i := \{y_1^i, y_2^i, y_3^i, \dots\}$, $i = 1, \dots, 5$, using recursive formula involving slow divergence integrals, as described in Section 1. For the initial value y_1^i, we use the value of y_0 multiplied by a factor κ_i depending on a test case, see Table 1. So for each example system we present five test cases involving different initial values $y_1^i = y_0 \cdot \kappa_i$. Idea is to demonstrate the independence of the box dimension of the choice of the initial point y_1^i.

test case i	1	2	3	4	5
factor κ_i	$1 - 10^{-16}$	$1 - 10^{-8}$	$1 - 10^{-4}$	$1 - 10^{-2}$	$1 - 10^{-1}$

Table 1: Factors κ_i.

We first normalize orbits $\mathcal{O}^i$. For each $\mathcal{O}^i$ we define normalized orbit $\tilde{\mathcal{O}}^i := \{x_1^i, x_2^i, x_3^i, \dots\}$, using $x_n^i = y_0 - y_n^i$. Notice that $\dim_B \tilde{\mathcal{O}}^i = \dim_B \mathcal{O}^i$, as box dimension of a set is invariant to any isometric map (in our case to translation and reflection). Orbit $\tilde{\mathcal{O}}^i$ tends monotonically to zero from the right side.

For calculating the box dimension, we use the formula from [18],

$$\dim_B \tilde{\mathcal{O}}^i = \lim_{\delta \to 0} \left(1 - \frac{\log |U_\delta^i|}{\log \delta} \right), \tag{8}$$

where by putting $U^i = \tilde{\mathcal{O}}^i$, the value $|U^i_\delta|$ is the Lebesgue measure of U^i_δ, that is the δ-neighborhood of orbit $\tilde{\mathcal{O}}^i$. It is easy to see that $|U^i_\delta|$ viewed as a real function of variable δ, where $\delta > 0$, is a continuous function. Now, define sequence $(\delta^i_n)_n$ with $\delta^i_n = (x^i_n - x^i_{n+1})/2 > 0$. Sequence $(\delta^i_n)_n$ tends monotonically to zero (see the proof of Theorem 1), so from (8) follows that

$$\dim_B \tilde{\mathcal{O}}^i = \lim_{n\to\infty} \left(1 - \frac{\log \left| U^i_{\delta^i_n} \right|}{\log \delta^i_n} \right). \tag{9}$$

The problem is in the numerical calculation of the limit in the formula (9), as $n \to \infty$. Notice that, as we are numerically computing the orbit $\tilde{\mathcal{O}}^i$, we can always only calculate some finite number M, of points x^i_n in the orbit $\tilde{\mathcal{O}}^i$. To compute $|U^i_{\delta^i_n}|$, we follow idea from the proof of Theorem 1, derived from [18], about decomposing δ-neighborhood into tail and nucleus. We compute

$$\left| U^i_{\delta^i_n} \right| = \left| T^i_{\delta^i_n} \right| + \left| N^i_{\delta^i_n} \right| = 2\delta^i_n n + (x^i_{n+1} + 2\delta^i_n) = (n+1)x^i_n - n x^i_{n+1},$$

see Fig. 3, respecting that in this chapter sequence $(x_n)_n$ is indexed starting with 1. Finally, to numerically estimate the box dimension of orbit $\mathcal{O}^i$, which is equal to $\dim_B \tilde{\mathcal{O}}^i$, we approximate the limit from (9). There, we take $n = M-1$, so we get formula

$$\dim_B \mathcal{O}^i \approx 1 - \frac{\log \left(M x^i_{M-1} - (M-1) x^i_M \right)}{\log \left(\left(x^i_{M-1} - x^i_M \right)/2 \right)}. \tag{10}$$

5.2 Implementation details

Regarding Wolfram Mathematica implementation, we use a combination of functions 'NIntegrate' for numerical integration and 'FindRoot' for root-finding using Newtons method. Although, slow divergence integrals could be symbolically evaluated in the case where functions H, F and G are polynomials, in regard to robustness of our numerical method, we choose to exclusively use numerical integration.

Sufficient precision in all numerical calculations is very important, since values in orbits $\mathcal{O}^i$ can converge exponentially fast. It means that in formula (10), values of x^i_{M-1} and x^i_M can get very close. To get a meaningful numerical estimate of the box dimension, precision significantly greater than standard double precision is needed. That is why we used Mathematica's ability to perform arbitrary precision calculation. Increased precision nonlinearly increases the time needed for numerical integration and root-finding. To make calculations last no longer than a few hours on a desktop computer, we managed to calculate only first 500 to 10000 values in orbits $\mathcal{O}^i$, depending on a specific example. This proved to be sufficient to calculate numerical estimates of box dimensions, only to a few percent difference than our theoretical expectation (see Table 2).

Also take into consideration that because of simplicity of presentation, all numerical values written in this paper are given only up to 6 decimal digits of precision. This remark is especially important in Section 5.4.

5.3 Slow-fast Liénard equation of type (2,4)

We consider the slow-fast system

$$\left\{ \begin{array}{rcl} \dot{x} & = & y - \frac{1}{2}x^2 \\ \dot{y} & = & \epsilon(b_0 - x - 0.5x^2 + x^4), \end{array} \right. \tag{11}$$

where $(\epsilon, b_0) \sim (0,0)$, and using the box dimension method we prove:

- *For each $\epsilon > 0$ and $\epsilon \sim 0$, system (11) contains a saddle-node bifurcation of limit cycles when we vary the breaking parameter $b_0 \sim 0$.*

The slow dynamics of (11) along the critical curve $\{y = \frac{1}{2}x^2\}$, given by $x' = -1-0.5x+x^3$, is strictly negative for all $x \in]-x_0, x_0[$, where $x_0 > 0$ is the simple zero of the slow dynamics. Following Theorem 3 of [13], it suffices to detect a balanced canard cycle Γ_{y_0} with the trivial box dimension, where $y_0 \in]0, \frac{1}{2}x_0^2[$. Thus, we generate an orbit $\mathcal{O} = \{y_1, y_2, y_3, \dots\}$ of y_1 ($y_1 \sim y_0$ and $y_1 \neq y_0$) by using the following equation:

$$\int_{-\sqrt{2y_{n+1}}}^{\sqrt{2y_n}} \frac{\rho d\rho}{-1 - 0.5\rho + \rho^3} = 0, \quad n \geq 1,$$

and numerically compute $\dim_B \mathcal{O}$, see Table 2 and Figure 4. Trivial box dimension induces exponential convergence of orbit, so we had to use arbitrary precision calculations of up to 170 decimal digits, and with only the first $M = 500$ values calculated.

example system	(11)	(12)	(13)
theoretical box dim.	0	1/2	0
num. of digits of prec.	170	60	150
computed orbit size M	500	10000	2000
test case 1 box dim.	0.019946	0.499413	0.031357
test case 2 box dim.	0.021066	0.498836	0.033703
test case 3 box dim.	0.021675	0.521252	0.035013
test case 4 box dim.	0.021993	0.532500	0.035706
test case 5 box dim.	0.022166	0.532658	0.036062

Table 2: Numerically computed box dimensions.

5.4 Slow-fast Liénard equation of type (2,6)

Let's consider now the following slow-fast Liénard equation of degree 6:

$$\left\{ \begin{array}{rcl} \dot{x} & = & y - \frac{1}{2}x^2 \\ \dot{y} & = & \epsilon(b_0 - x + \mu_2 x^2 + \mu_3 x^3 + \mu_4 x^4 + \mu_5 x^5 + x^6), \end{array} \right. \tag{12}$$

where $(\epsilon, b_0) \sim (0,0)$ and $(\mu_2, \mu_3, \mu_4, \mu_5) \sim (1.004468, 0, -2.189363, 0)$. Like in Section 5.3, we use the box dimension algorithm, and we show that:

- *System (12) has at most* 3 *limit cycles Hausdorff close to* Γ_{y_0}*, for all* $y_0 \sim 0.767488$*,* $\epsilon > 0$*,* $\epsilon \sim 0$*,* $b_0 \sim 0$ *and* $(\mu_2, \mu_3, \mu_4, \mu_5) \sim (1.004468, 0, -2.189363, 0)$*.*

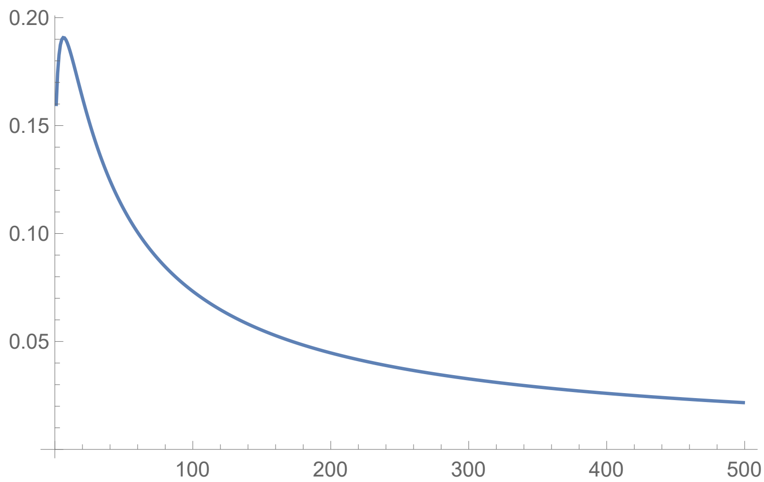

Figure 4: The numerical estimate of the box dimension depending on the number of calculated orbit values M, in system (11) and test case 3.

It suffices to prove that the box dimension of Γ_{y_0} is equal to $\frac{1}{2}$, for $y_0 = 0.767488$ and $(\mu_2, \mu_3, \mu_4, \mu_5) = (1.004468, 0, -2.189363, 0)$ (see Theorem 2 of [13]). First, note that the slow dynamics of (12) is negative for all $x \in [-1.4, 1.4]$ and $(\mu_2, \mu_3, \mu_4, \mu_5) = (1.004468, 0, -2.189363, 0)$. We generate one orbit $\mathcal{O} = \{y_1, y_2, y_3, \dots\}$ of y_1 ($y_1 \sim 0.767488$ and $y_1 \neq 0.767488$) by using the following equation:

$$\int_{-\sqrt{2y_{n+1}}}^{\sqrt{2y_n}} \frac{\rho d\rho}{-1 + 1.004468\rho - 2.189363\rho^3 + \rho^5} = 0, \quad n \geq 1,$$

and we numerically compute $\dim_B \mathcal{O}$, see Table 2 and Figure 5. Here it was sufficient to use arbitrary precision calculations of up to 60 decimal digits, which proved to be fast enough for the first $M = 10000$ orbit values calculated. Notice that given numerical values in this example are not exact, but merely approximations up to the first 6 decimal places. Before attempting to recreate our numerical box dimension results, values of μ_2, μ_4 and y_0 should be recalculated up to sufficient precision.

5.5 Slow-fast Liénard equation of type (4,8)

In this section we focus on a slow-fast Liénard equation of degree 8 with cubic damping:

$$\left\{ \begin{array}{rcl} \dot{x} & = & y - (a_0 x + \frac{1}{2}x^2 - \frac{1}{4}x^4) \\ \dot{y} & = & \epsilon\big(b_0 - x - 0.05(x^2 - x^4 + x^6 - 0.5x^8)\big), \end{array} \right. \tag{13}$$

where $(\epsilon, a_0, b_0) \sim (0, 0, 0)$. Our goal is to prove the following statement by using the box dimension method for canard cycles with two breaking parameters:

- *System (13) undergoes a cusp-catastrophy of relaxation oscillations for each $\epsilon > 0$ and $\epsilon \sim 0$.*

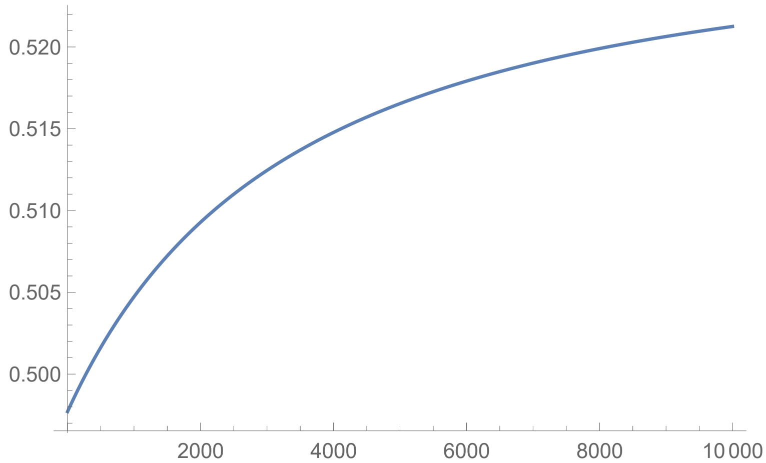

Figure 5: The numerical estimate of the box dimension depending on the number of calculated orbit values M, in system (12) and test case 3.

Suppose that $(a_0, b_0) = (0, 0)$. The critical curve of (13) is given by $\{y = \frac{1}{2}x^2 - \frac{1}{4}x^4\}$. The critical curve has two maxima of Morse type at $x = -1$ and $x = 1$, and it can be easily seen that the points $(x, y) = (-1, \frac{1}{4})$ and $(x, y) = (1, \frac{1}{4})$ form a jump breaking mechanism (see Assumption 2 in Section 1). Furthermore, the critical curve has a minimum of Morse type at $x = 0$ and the origin is a slow-fast Hopf point with the breaking parameter b_0 (see Assumption 3 in Section 1). The slow dynamics of (13) along the critical curve, away from the contact points, is given by

$$x' = \frac{-1 - 0.05(x - x^3 + x^5 - 0.5x^7)}{1 - x^2}.$$

It can be easily seen that the slow dynamics is regular on the interval $[-\sqrt{2}, \sqrt{2}] \setminus \{\pm 1\}$, i.e. $-1 - 0.05(x - x^3 + x^5 - 0.5x^7) < 0$ for all $x \in [-\sqrt{2}, \sqrt{2}]$ (see Assumption 4). Note that $x = \pm\sqrt{2}$ are two simple zeros of $y = \frac{1}{2}x^2 - \frac{1}{4}x^4$. The section $S = \{x = -1\}$ (resp. $T = \{x = 1\}$) is parametrized by $z \in]0, \frac{1}{4}[$ (resp. $w \in]0, \frac{1}{4}[$)

Following Theorem 4, we have to find a balanced canard cycle Γ_{z_0, w_0} of (13) with the trivial box dimension, for some $(z_0, w_0) \in]0, \frac{1}{4}[\times]0, \frac{1}{4}[$. We define (see (4))

$$\begin{cases} I_1(z) := \int_{-\sqrt{1+\sqrt{1-4z}}}^{-1} \Psi(x)dx, \ I_2(w) := -\int_1^{\sqrt{1+\sqrt{1-4w}}} \Psi(x)dx \\ I_3(z) := \int_{-\sqrt{1-\sqrt{1-4z}}}^{0} \Psi(x)dx, \ I_4(w) := -\int_0^{\sqrt{1-\sqrt{1-4w}}} \Psi(x)dx, \end{cases}$$

where $(z, w) \in]0, \frac{1}{4}[\times]0, \frac{1}{4}[$ and $\Psi(x) = \frac{x(1-x^2)^2}{1+0.05(x-x^3+x^5-0.5x^7)}$. Now, we generate one orbit $\tilde{\mathcal{O}} = \{z_1, z_2, z_3, \dots\}$ of z_1 ($z_1 \sim z_0$ and $z_1 > z_0$) by using the recursive formula $z_{n+1} = z_n - (w_n^2 - w_n^1)$, $n \geq 1$, where $w_n^1, w_n^2 \sim w_0$ are unique numbers with the property that $I_1(z_n) = I_2(w_n^1)$ and $I_3(z_n) = I_4(w_n^2)$. We numerically compute $\dim_B \tilde{\mathcal{O}}$, see Table 2 and Figure 6. Again, as we have trivial box

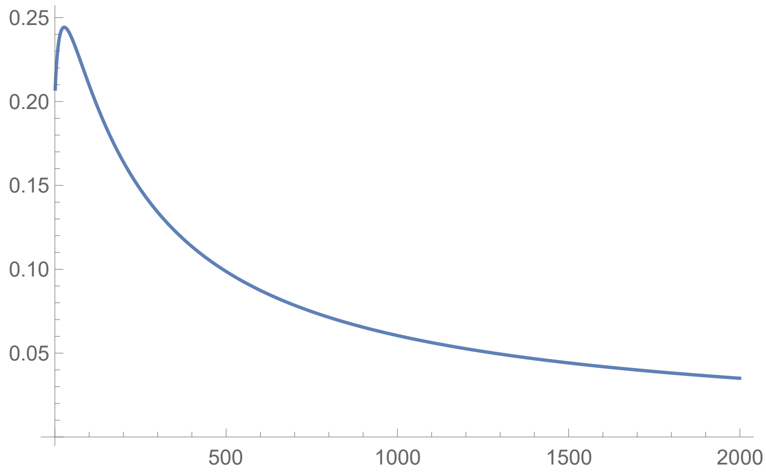

Figure 6: The numerical estimate of the box dimension depending on the number of calculated orbit values M, in system (13) and test case 3.

dimension, exponential convergence of the orbit happens, so arbitrary precision needed is 150 decimal digits. We calculated the first $M = 2000$ values of the orbit $\mathcal{O}$.

References

[1] E. Benoit. Équations différentielles: relation entrée–sortie. *C. R. Acad. Sci. Paris Sér. I Math.*, 293(5):293–296, 1981.

[2] P. De Maesschalck and F. Dumortier. Time analysis and entry-exit relation near planar turning points. *J. Differential Equations*, 215(2):225–267, 2005.

[3] P. De Maesschalck and F. Dumortier. Canard cycles in the presence of slow dynamics with singularities. *Proc. Roy. Soc. Edinburgh Sect. A*, 138(2):265–299, 2008.

[4] P. De Maesschalck and F. Dumortier. Classical Liénard equations of degree $n \geq 6$ can have $[\frac{n-1}{2}]+2$ limit cycles. *J. Differential Equations*, 250(4):2162–2176, 2011.

[5] P. De Maesschalck and R. Huzak. Slow divergence integrals in classical liénard equations near centers. *J Dyn Diff Equat*, DOI = 10.1007/s10884-014-9358-1, 2014.

[6] F. Diener and M. Diener. Chasse au canard. I. Les canards. *Collect. Math.*, 32(1):37–74, 1981.

[7] F. Dumortier. Slow divergence integral and balanced canard solutions. *Qual. Theory Dyn. Syst.*, 10(1):65–85, 2011.

[8] F. Dumortier, D. Panazzolo, and R. Roussarie. More limit cycles than expected in Liénard equations. *Proc. Amer. Math. Soc.*, 135(6):1895–1904 (electronic), 2007.

[9] F. Dumortier and R. Roussarie. Canard cycles and center manifolds. *Mem. Amer. Math. Soc.*, 121(577):x+100, 1996. With an appendix by Li Chengzhi.

[10] F. Dumortier and R. Roussarie. Canard cycles with two breaking parameters. *Discrete Contin. Dyn. Syst.*, 17(4):787–806, 2007.

[11] N. Elezović, V. Županović, and D. Žubrinić. Box dimension of trajectories of some discrete dynamical systems. *Chaos Solitons Fractals*, 34(2):244–252, 2007.

[12] K. Falconer. *Fractal geometry.* John Wiley and Sons, Ltd., Chichester, 1990. Mathematical foundations and applications.

[13] R. Huzak. Box dimension and cyclicity of canard cycles. *Qual. Theory Dyn. Syst. (2017). https://doi.org/10.1007/s12346-017-0248-x.*

[14] S. G. Krantz and H. R. Parks. *The geometry of domains in space.* Birkhäuser Advanced Texts: Basler Lehrbücher. [Birkhäuser Advanced Texts: Basel Textbooks]. Birkhäuser Boston, Inc., Boston, MA, 1999.

[15] M. Krupa and P. Szmolyan. Relaxation oscillation and canard explosion. *J. Differential Equations*, 174(2):312–368, 2001.

[16] L. Mamouhdi and R. Roussarie. Canard cycles of finite codimension with two breaking parameters. *Qual. Theory Dyn. Syst.*, 11(1):167–198, 2012.

[17] P. Mardešić, M. Resman, and V. Županović. Multiplicity of fixed points and growth of ε-neighborhoods of orbits. *J. Differential Equations*, 253(8):2493–2514, 2012.

[18] C. Tricot. *Curves and fractal dimension.* Springer-Verlag, New York, 1995. With a foreword by Michel Mendès France, Translated from the 1993 French original.